Ioffe Institute
6th Int. Symp. "Nanostructures: Physics and Technology"
St Petersburg, Russia, June 22–26, 1998.

Absorption coefficient of InGaAs V-shaped quantum wires integrated in optical waveguides by MBE growth

F. Filipowitz†, C. Gourgon†, D. Martin†, Y. Magnenat†, P. Giaccari†, F. Bobard‡ and F. K. Reinhart†
† Institute of Micro- and Optoelectronics
‡ Center of Electron Microscopy
Federal Institute of Technology, CH-1015 Lausanne, Switzerland

Abstract. Optical waveguides with InGaAs quantum wires grown by MBE integrated in the middle of their core are investigated. Photocurrents induced by guided TE and TM modes propagating parallel or perpendicular to the quantum wires have been measured and reflect the anisotropy of the optical matrix element. Spectra of the transmitted intensity of these guided modes have been measured, and the attenuation coefficient of the guided modes due to band edge optical absorption in the quantum wire is established. The attenuation coefficient and the evaluation of the overlap integral between the active material and the optical intensity permits to evaluate, for the first time, the absorption coefficient of these quantum wires.

1 Introduction

Due to the Van Hove singularity in the density of states, quantum wires (QWR) are thought to be good candidates for future modulators [1]. The fabrication steps to obtain high quality V-shaped GaAs QWR embedded in AlAs/GaAs superlattices on a GaAs substrate by molecular beam epitaxy (MBE) are reproducibly controlled [2]. The next step toward possible application, the integration of InGaAs QWR [3] in optical waveguides is achieved [4]. The evaluation of the attenuation coefficient [5] of guided mode propagating in optical waveguides that contains QWR is a direct evaluation of the potential possibilities of such modulators. Four different waveguides were grown to realize this evaluation, two contain InGaAs QWR of different sizes, one contains an InGaAs quantum well (QW) and one contains the barriers of the QW without any InGaAs deposition.

2 Sample fabrication and TEM observation

The fabrication of waveguides that contains QWR consists of three process sequences: (i) MBE growth of the lower waveguide cladding and half of the waveguide core, (ii) patterning of the core by deep UV holographic lithography and wet chemical etching, (iii) MBE growth of the lower barrier, QWR, higher barrier, second part of the core and the upper cladding.

If the lowest energy interband optical transition of the integrated QWR has a higher energy then the band gap of the materials that constitute the waveguide, the variations of transmitted intensities and induced photocurrents of guided modes due to the QWR are drowned in the variations due to the waveguide materials. The QWR must therefore have the lowest band gap among all the materials that constitute the waveguide. We

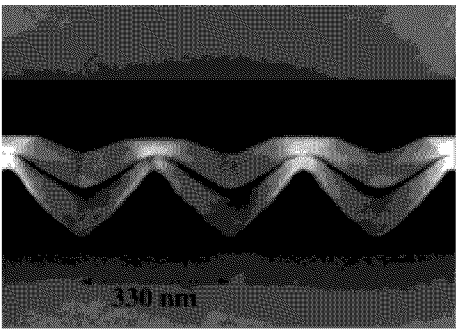

Fig. 1. TEM micrograph sample A.

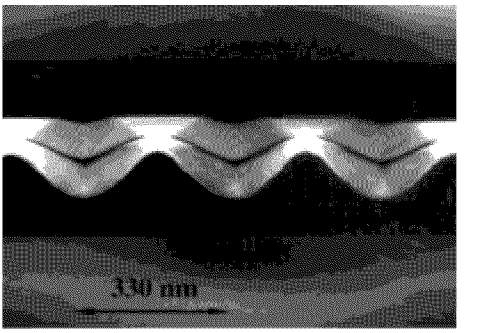

Fig. 2. TEM micrograph sample B.

first tried to integrate the widely studied [6–9] GaAs QWR in AlGaAs waveguides. The high dislocations density due to MBE regrowth over a non planar AlGaAs surface forced us to find another solution. Despite the lattice mismatch between $In_{0.16}Ga_{0.84}As$ and GaAs, fabrication of InGaAs QWR [3] with the same photoluminescence signals as the GaAs QWR is now reproducibly achieved. Furthermore the bandfilling effects observed at low excitation density on GaAs QWR [6] are also observed [4] with InGaAs QWR.

Figures 1 and 2 show transmission electron microscopy (TEM) micrographs of samples A and B, respectively. $In_{0.16}Ga_{0.84}As$ QWR are surrounded by a 20 periods superlattice $(AlAs)_4/(GaAs)_8$ one each side. They are in the approximative center of a GaAs waveguide core (black color on the micrograph). The 0.4 μm thick GaAs core is surrounded by 2 μm $Al_{0.15}Ga_{0.85}As$ claddings, partly visible on the micrograph. The growth was realized on a n-type GaAs substrate. The QWR, core, superlattice and 0.4 μm of the upper and lower claddings adjacent to the core are nominally undoped. The rest of the lower (upper) cladding is nominally n-doped (p-doped) with 5×10^{17} Si (Be) impurities. The QWR integrated in sample A (B) were fabricated by the deposition of a 45 Å(34 Å) $In_{0.16}Ga_{0.84}As$ QW over a non planar GaAs core. The QWR are embedded in a $(AlAs)_4/(GaAs)_8$ superlattice for two reasons: (i) to remove them from the regrowth interface to avoid defects and impurities in the QWR and (ii) to provide higher barriers to improve the confinement of electrons and especially holes in the QWR. Samples C and D were grown to compare results obtained on sample A and B with more conventional structures. A 60 Å thick $In_{0.16}Ga_{0.84}As$ QW, surrounded by a 20 periods superlattice $(AlAs)_4/(GaAs)_8$ one each side, was deposited in the middle of the 0.4 μm GaAs core of sample C. The rest of the structures and the nominal doping profile are identical to samples A and B. Sample D is similar to sample C, except that no InGaAs was deposited. Samples C and D were grown with a single growth sequence, as no non planar structuration was necessary. The optical waveguides were designed to support only the fundamental transverse electric (TE) and transverse magnetic (TM) guided mode at a wavelength of 0.9 μm.

Ohmic contacts were deposited on both side of the diode. Capacitance–voltage (C–V) measurements realized on samples A–D indicate that the growth interruption did not modify the electrical behavior of these pin diodes.

Electrons can move freely along the [011] crystallographic direction. The growth direction, [100], is the strong confinement direction, electrons are less confined along

[01$\bar{1}$], usually called the lateral confinement direction. Comparing Fig. 1 and Fig. 2, the bigger size of the QWR of sample A is easily observed. Differences in the profile of the lower part of the GaAs core are explained in [4]. The absence of dislocations indicates the good efficiency of the desorption prior to the regrowth.

3 Photocurrent spectra

The probability that a photon induces an electronic transition between valence and conduction band is, in the dipole approximation, proportional to the square of the optical dipole matrix element, $|\langle f|\mathbf{e}\cdot\mathbf{p}|i\rangle|^2$ where f(i) is the conduction (valence) band state, $\mathbf{p}$ the momentum operator and $\mathbf{e}$ a unitary vector in the direction of the optical electrical field. Standard polarized photoluminescence (PL) and photoluminescence excitation made on QWR are possible for $\mathbf{e}$ aligned along two orthogonal directions only. The advantage of the integration of QWR in planar waveguide is the possibility to realize measurements with $\mathbf{e}$ aligned along three orthogonal directions. We have measured photocurrents induced by guided TM or TE modes excited by light propagating along the [011] or [01$\bar{1}$] direction using edge coupling. The light was generated by a tungsten filament and passes through a monochromator. The optical power at the monochromator exit slot is approximately 1 nW for a bandwidth of 1 nm. Results of measurements made on sample A are shown in Fig. 3 for TM modes and in Fig. 4 for TE modes. Significative photocurrents are obtained at forward bias in the range of 0.2 to 1 volt. The intensity of the photocurrent strongly depends on the applied bias, not the profile of the spectra. Due to the fact that different diodes of samples A and B were used, it will be difficult to compare photocurrent spectra on a absolute scale. The direction of the optical electrical field of TM modes is nearly parallel to the [100] direction independently of the propagation direction. The direction of the optical electrical field of a TE mode depends on the propagation direction of the mode. It is aligned along [011] ([01$\bar{1}$]) if the TE mode propagates along [01$\bar{1}$] ([011]). The photocurrent generated by the guided light is proportional to the number of absorbed photons per unit time for low light level. In this case the photocurrent is also proportional to the square of the optical matrix element of the QWR. The qualitatively different features of the photocurrents spectra are presented in Fig. 3 and Fig. 4 and reflect the anisotropy of the optical matrix element of QWR.

At the same photon energy that the photocurrent peak induced by TM modes, qualitatively different photocurrent spectra are induced by TE modes that propagate along [011] or [01$\bar{1}$]. These qualitatively different photocurrent spectra are well explained by the expected anisotropy of the optical matrix element of QWR [10].

The photocurrent spectra of sample B (not shown here) have the same features as those shown on Fig. 3 and Fig. 4. They are only shifted in energy. Sample D showed no significative photocurrent in the 900–1000 nm range.

This is the first time that the anisotropy of the optical matrix element of transitions induced by an electrical optical field aligned along [100] is observed with our technique.

4 Transmission spectra

Spectra of the transmitted intensity of guided modes are under investigations. At the same photon energy, the decrease of the transmitted intensity corresponds to the increase of the photocurrent intensity and to the lowest energy photoluminescence peak of the

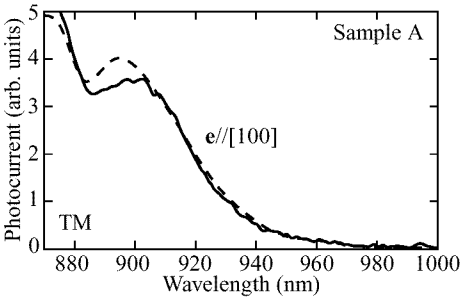

Fig. 3. Photocurrent induced by TM modes propagating either along [011] (dotted line) or along [01$\bar{1}$] (solid line). The direction of the optical electrical field, **e**, is indicated.

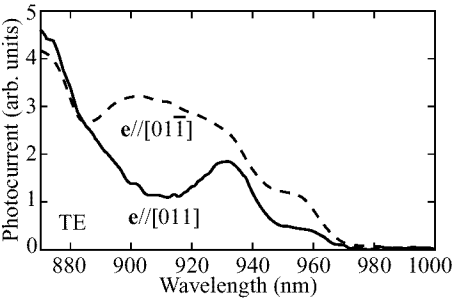

Fig. 4. Photocurrent induced by TE modes propagating either along [011] (dotted line) or along [01$\bar{1}$] (solid line). The direction of the optical electrical field, **e**, is indicated.

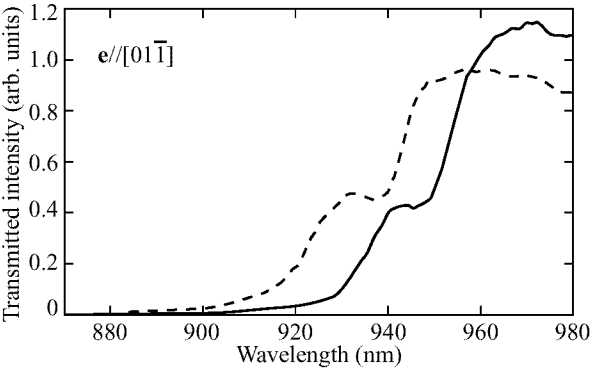

Fig 5. Transmitted intensity of TE modes propagating along [011] in sample A (solid line) or sample B (dotted line).

QWR. This observation establishes that the attenuation of the guided mode is due to band edge optical absorption in the QWR. An estimation of the absorption coefficient of QWR, α_{QWR}, can be deduced from the experimental determination of the attenuation coefficient, α_{att}, of the guided mode and the evaluation of the overlap integral between the active material and the optical intensity, Γ, using the relation $\alpha_{att} \cong \Gamma\alpha_{QWR}$.

Spectra of the transmitted intensity of guided modes are realized with a continuous wave operation Ti-Sapphire Laser with a linewidth of about 40 GHz. The optical power at the Ti-Sapphire exit was approximately 1 mW. Figure 5 shows spectra of guided TE modes propagating along [011] in samples A and B. In the case of sample A, the decrease between 950–960 nm and 930–940 nm corresponds to photocurrent peaks, shown in Fig. 4, around 955 nm and 932 nm, respectively. Furthermore the lowest energy photocurrent peak correspond to the lowest energy peak observed in PL measurements. The same correspondence between decrease of the transmitted intensity, photocurrent increase and PL peaks can be made with sample B. The energy shift between the two spectra shown in Fig. 5 is due to the difference of the QWR size. The attenuation coefficient associated with the fundamental transition observed by the

TE mode propagating along [011] in sample A (B) is estimated to be $\alpha_{att} \approx 6\,cm^{-1}$ ($\alpha_{att} \approx 5.5\,cm^{-1}$). A rough estimation of the overlap factor gives $\Gamma \cong 0.24\%$ (0.18%), thus the absorption coefficient of QWR is in the range of: $\alpha_{QWR} \cong 2.5{-}3 \times 10^3\,cm^{-1}$. This low value has to be confirmed by further experiments.

The low absorption coefficient of QWR is in agreement with the lower attenuation coefficient observed for guided modes propagating in sample A or B as compared to the guided modes propagating in sample C.

5 Conclusion

The absorption coefficient of QWR has been experimentally evaluated for the first time by direct measurement of transmission changes at the band edge. The low value of this absorption coefficient is in contradiction with simple theoretical expectations [1]. Photocurrent spectra show the expected anisotropy of the optical matrix element of QWR [10].

References

[1] D.A.B. Miller, D.S. Chemla and S. Schmitt-Rink, *Appl. Phys. Lett.* **52** 2154 (1988).
[2] U. Marti, M. Proctor, D. Martin, F. Morier-Genoud, B. Senior and F.K. Reinhart, *Microelectr. Eng.* **13** 391 (1991).
[3] P.H. Jouneau, F. Bobard, U. Marti, J. Robadey, F. Filipowitz, D. Martin, F. Morier-Genoud, P.C. Silva, Y. Magnenat and F.K. Reinhart, *Inst. Phys. Conf. Ser.* **146** 371 (1995).
[4] C. Gourgon, F. Filipowitz, J. Robadey, D. Martin, Y. Magnenat, P.C. Silva, F. Bobard and F.K. Reinhart, this conference, (1998).
[5] R.G. Hunsperger, *Integrated Optics: Theory and Technology*, Springer Series in Optical Sciences, 3rd ed. (1991).
[6] R. Rinaldi, M. Ferrara, R. Cingolani, U. Marti, D. Martin, F. Morier-Genoud, P. Ruterana and F.K. Reinhart, *Phys. Rev. B* **50** 11795 (1994).
[7] R. Rinaldi, P.V. Giugno, R. Cingolani, F. Rossi, E. Molinari, U. Marti and F.K. Reinhart, *Phys. Rev. B* **53** 13710 (1996).
[8] R. Rinaldi, R. Cingolani, M. Lepore, M. Ferrara, I.M. Catalano, R. Cingolani, F. Rossi, L. Rota, E. Molinari, P. Lugli, U. Marti, D. Martin, F. Morier-Genoud, P. Ruterana and F.K. Reinhart, *Phys. Rev. Lett.* **73** 2899 (1994).
[9] F. Rossi and E. Molinari, *Phys. Rev. Lett.* **76** 3642 (1996).
[10] F. Filipowitz and F.K. Reinhart, *Helv. Phys. Acta* **70** (1997).